Correspondence

Enhanced Ultrasonic Imaging with Split-Spectrum Processing and Polarity Thresholding

NIHAT M. BILGUTAY, UTHAI BENCHARIT, AND JAFAR SANIIE

Abstract—**Coherent noise resulting from a large number of complex and randomly distributed scatterers which often masks the target echo is a fundamental limitation affecting many imaging and detection applications. This correspondence examines the polarity thresholding algorithm, which utilizes the frequency decorrelation principle based on the split-spectrum processing technique developed in earlier work. Split-spectrum processing obtains an ensemble of frequency diverse signals from a wide-band received signal by using a set of parallel bandpass filters with different center frequencies. Polarity thresholding acts as an on–off switch on the resulting data by setting the output to zero at time instants where the split-spectrum ensemble exhibits polarity reversal. Since the target echo will exhibit significantly smaller variation with frequency compared to clutter echos, polarity thresholding will maintain the target echo while suppressing a significant portion of the clutter echos. Theoretical derivations are provided to determine the signal-to-noise ratio enhancement capabilities of the algorithm. Ultrasonic data obtained from large-grained stainless steel samples with flat-bottom holes are used to verify the theoretical results and demonstrate the grain echo suppression capability of the algorithm in imaging applications.**

Introduction

Clutter is a common problem which affects a wide range of applications in radar, optics, and ultrasound, and cannot be effectively suppressed by conventional time averaging. However, in practice, it is possible to decorrelate the clutter by using diversity techniques which shift either the transmitted frequency or the position of the transmitter/receiver without adversely affecting the target echo [1]. Consequently, processing the resulting signal ensemble can improve the signal-to-noise (clutter) ratio. The split-spectrum processing (SSP) technique was originally developed in ultrasonic nondestructive testing to achieve frequency diversity at the receiver while transmitting a single wide-band signal. The received signal spectrum is partitioned into different frequency bands using a bank of parallel bandpass filters to obtain a set of narrow-band signals with decorrelated clutter [2]–[5]. Noise suppression algorithms can then be applied to the resulting data to enhance the target signal. Thus, SSP eliminates the need for complex modulation techniques or multiple transmitters to achieve frequency diverse signals. Furthermore, a different set of decorrelated data can be obtained conveniently from the original data by using a new set of window parameters. Because of its effectiveness and versatility, the SSP technique has been widely utilized both in nondestructive testing and imaging applications [2]–[5].

Manuscript received January 12, 1988; revised January 3, 1989. This work was supported in part by NSF Grant ECS-8505153 and by the SDIO/IST funds managed by the Office of Naval Research under Contract N00014-86-K-0520.

N. M. Bilgutay and U. Bencharit are with the Department of Electrical and Computer Engineering, Drexel University, Philadelphia, PA 19104.

J. Saniie is with the Department of Electrical and Computer Engineering, Illinois Institute of Technology, Chicago, IL 60616.

IEEE Log Number 8930015.

This correspondence will examine the polarity thresholding (PT) algorithm, which is used in conjunction with the SSP technique, first theoretically to determine its performance in terms of signal-to-noise ratios and later experimentally. Large grained stainless steel samples with flat-bottom holes were tested to evaluate the effectiveness of the algorithm in suppressing grain noise (clutter) with respect to the flaw (target) signal.

Theoretical Results for the Polarity Thresholding Algorithm

The PT algorithm is based on the principle that at time instants where the flaw signal is present, the corresponding SSP data set will not exhibit any polarity reversal since the flaw signal will dominate the grain noise (i.e., all the elements of the corresponding column will have the same polarity). However, if the data set contains only grain noise, which is zero mean, then it is likely that the data will exhibit polarity reversal. Therefore, by setting the amplitude of the processed signal to zero at time instants where polarity reversal occurs while maintaining the original value of the unprocessed wide-band signal when the data have identical polarity, the grain noise level can be reduced significantly. Therefore, the PT output can be expressed as

$$y_{PT}(t_k) = \begin{cases} r(t_k) & \text{if } r_i(t_k) > 0 \text{ or } r_i(t_k) < 0 \\ & \text{for all } i = 1, 2, \cdots, N \\ 0 & \text{otherwise} \end{cases} \quad (1)$$

where t_k are discrete time instants with $k = 1, 2, \cdots, M$.

The SNR derivations for the PT algorithm will assume that the available spectral region is split into N independent and nonoverlapped bands using rectangular windows. This assumption affords mathematical simplicity in the analysis of the algorithm without loss of generality. Since the received wide-band signal $r(t)$ is assumed to be a random process, its value at a particular time instant $t = t_0$ will be a random variable $r = r(t_0)$. The SNR derivations are based on the following hypothesis testing model where the observation time $t = t_0$ is assumed to coincide with the peak value of the defect echo (when defect is present) so that the observed signal may be represented as

$$\begin{aligned} H_1&: r = m + n \quad \text{defect present} \\ H_0&: r = n \quad \text{no defect} \end{aligned} \quad (2)$$

where m is the peak value of the flaw echo and n is the zero-mean Gaussian random variable with variance σ^2 representing the grain noise component. Note that the "flaw" component is represented by a nonrandom amplitude m, while the "noise" component for hypotheses H_1 and H_0 is represented by a random variable n. The SNR is defined as [3]

$$\text{SNR} = \frac{E[r|H_1]}{\text{rms}\,[r|H_0]} \quad (3)$$

where $E[\,]$ and rms denote the expected and the root-mean-square values, respectively. Therefore, from (2) and (3), the input SNR becomes

$$(\text{SNR})_{\text{in}} = \frac{E[m+n]}{\text{rms}\,[n]} = \frac{m}{\sqrt{[E(n^2)]}} = \frac{m}{\sigma}. \quad (4)$$

Since the noise term n is zero-mean, its standard deviation and rms values are identical. The SNR at the output of the PT algorithm

0096-3518/89/1000-1590$01.00 © 1989 IEEE

using (3) becomes

$$SNR\big|_{PT} = \frac{E[y|H_1]}{\text{rms}\,[y|H_0]} \tag{5}$$

where y is the output of the PT algorithm. The application of split-spectrum processing to the unprocessed wide-band waveform using nonoverlapped rectangular windows results in an ensemble of independent and identically distributed (iid) narrow-band waveforms $r_i(t)$; $i = 1, 2, \cdots, N$, with bandwidths N times smaller than the original wide-band signal. Hence, both the flaw amplitude and the noise variance will reduce by a factor of N. Therefore, the numerator and denominator in (5) can be determined directly from the input statistics by using basic probability concepts as follows.

Since the input data which exhibit polarity reversal are set to zero, the mean value of the PT output will be equal to the mean value of the input times the probability of *no polarity reversal*, $P(\text{NPR})$. Therefore, for hypothesis H_1, the mean value of PT output becomes

$$E[y|H_1]\big|_{PT} = P(\text{NPR}|H_1)E[y|H_1]\big|_{In} \tag{6}$$

where the probability of detection P_D can be calculated as [3], [4]

$$P_D = P(\text{NPR}|H_1) = P(r_i \geq 0, \quad \text{for all } i\,|H_1) + P(r_i \leq 0, \quad \text{for all } i\,|H_1) \tag{7}$$

$$= \left[\frac{1}{2} + \frac{1}{2}\,\text{erf}\left(\frac{k}{\sqrt{N}}\right)\right]^N + \left[\frac{1}{2} - \frac{1}{2}\,\text{erf}\left(\frac{k}{\sqrt{N}}\right)\right]^N \tag{8}$$

where

$$\text{erf}\,(x) = \frac{2}{\sqrt{\pi}}\int_0^x e^{-u^2}\,du \quad \text{and} \quad k = \frac{m}{\sqrt{2}\sigma}. \tag{9}$$

Note that if one or more phase reversals occur for H_1, the output will be set to zero, which corresponds to the probability of miss $P_M = 1 - P_D$. Using the above argument, the noise power at the PT output will be equal to the input noise power times the probability of *no polarity reversal*. Therefore, for hypothesis H_0, the rms value of PT output becomes

$$\text{rms}\,[y|H_0]\big|_{PT} = [P(\text{NPR}|H_0)]^{1/2}\,\text{rms}\,[y|H_0]\big|_{In} \tag{10}$$

where the probability of false alarm P_{FA} can be calculated as [3], [4]

$$P_{FA} = P(\text{NPR}|H_0) = P(r_i \geq 0, \quad \text{for all } i\,|H_0) + P(r_i \leq 0, \quad \text{for all } i\,|H_0)$$

$$= 2(1/2)^N = 2^{(1-N)}. \tag{11}$$

Using the above results and (5), the SNR for PT becomes

$$(\text{SNR})\big|_{PT} = \frac{E[y|H_1]}{\text{rms}\,[y|H_0]} = \frac{P(\text{NPR}|H_1)}{[P(\text{NPR}|H_0)]^{1/2}}\,(\text{SNR})\big|_{In}. \tag{12}$$

Therefore, the signal-to-noise ratio enhancement for PT becomes

$$(\text{SNRE})\big|_{PT} = (\text{SNR})\big|_{PT}/(\text{SNR})\big|_{In} \tag{13}$$

$$(\text{SNRE})\big|_{PT} = \frac{\left[1 + \text{erf}\left(\frac{m}{\sqrt{2N}\sigma}\right)\right]^N + \left[1 - \text{erf}\left(\frac{m}{\sqrt{2N}\sigma}\right)\right]^N}{2^{(N+1)/2}}. \tag{14}$$

The $\text{SNRE}|_{PT}$ curves using (14) are plotted in Fig. 1(a) as a function of the number of windows N for different input SNR values (m/σ). It is evident from these curves that the performance of the PT algorithm shows sensitivity to the input SNR and the number of windows. The peak SNRE value (for a given input SNR) corresponds to the optimum choice of N, which in turn determines the optimum window bandwidth and reflects the best tradeoff between probability of detection (P_D) and the probability of false alarm (P_{FA}). The SNRE curves peak at higher N (i.e., smaller optimum window bandwidth) values as the input SNR increases. Finally, due to the nonlinear nature of the algorithm, the theoretical SNRE shows a more rapid improvement as the input SNR increases.

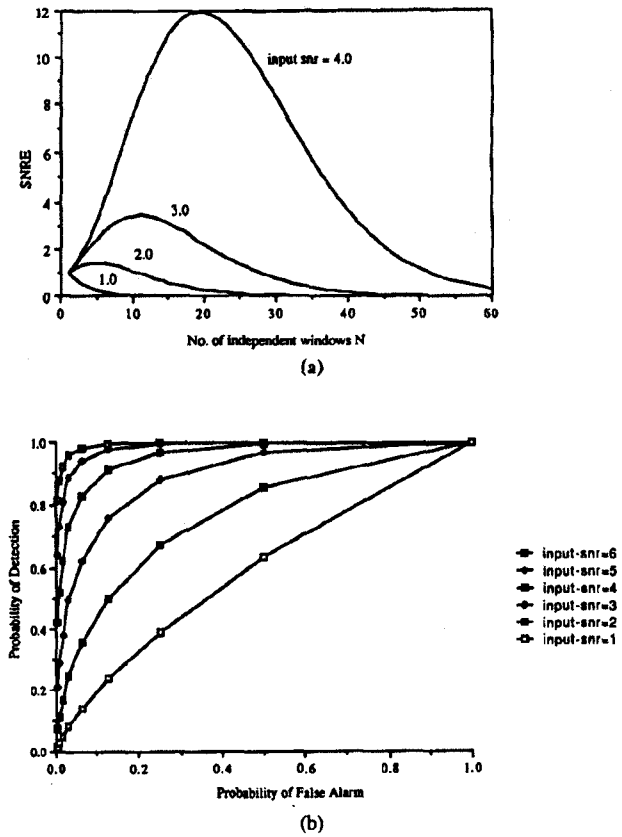

Fig. 1. Theoretical performance analysis for PT algorithm. (a) SNRE curves. (b) Receiver operating characteristics.

Analysis of simulated signals indicates that due to the random interference effects between the flaw and grain echos, SNR values of even 4 generally yield a combined signal where the grain echos are of similar amplitude as the flaw signal, such that it is difficult to distinguish between the two. Therefore, it is evident from the theoretical results of Fig. 1(a) that the PT algorithm can yield significant SNRE, even when the flaw signal is completely masked by the grain echos.

As an alternative approach to evaluating the performance of the PT algorithm, the receiver operating characteristic curves are plotted in Fig. 1(b) with the input SNR as a parameter. The probability of detection and the probability of false alarm are given by (8) and (11), respectively. As N increases, the probability of false alarm is seen to decrease much more rapidly than the probability of detection, especially as input SNR increases.

Experimental Results for the PT Algorithm

The PT algorithm was experimentally tested using type 303 heat-treated austenitic stainless steel samples with flat-bottom holes representing the flaw. Both A-scan and B-scan data were utilized experimentally. An A-scan is a 1-D plot obtained at a single test point (i.e., received signal amplitude versus time), whereas a B-scan is

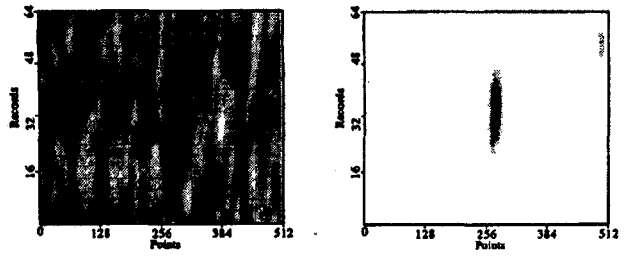

Fig. 2. Experimental results for SST75.

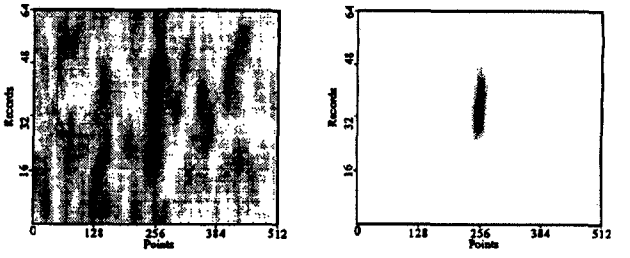

Fig. 3. Experimental results for SST50.

a 2-D representation obtained by combining *A*-scans from equally spaced points along a test line. The *B*-scan images displayed here use 256 gray levels. The experimental data were obtained using a 1/2 in diameter 5 MHz unfocused KB-Aerotech Alpha transducer with the scan plane parallel to the flat-bottom hole surface. The images presented here are comprised of 64 equally spaced (0.375 mm) *A*-scans, each consisting of 512 data points obtained at a sampling frequency of 50 MHz. It should be noted that the 2-D spectrum will consist of temporal frequency in the axial direction and spatial frequency in the lateral direction. The *B*-scan SSP technique uses 2-D format for all operations (i.e., FFT's and windows are two dimensional).

The unprocessed image for the SST75 sample, which has a 4.2 mm diameter flat-bottom hole located at 67.1 mm depth and an average grain size of 106 μm, is shown in Fig. 2(a). The received wide-band spectrum is partitioned into spectral bins using 2-D Gaussian windows with elliptical footprints which are symmetrically located in all four quadrants. The windows are generally overlapped to preserve the available information in the original image. The inverse 2-D FFT is performed on each frequency bin to obtain the spectrally decorrelated images which are then processed using the PT algorithm.

There are basically three interdependent processing parameters governing the performance of the algorithm: 1) spectral region over which SSP is performed, 2) window bandwidth, and 3) window spacing (i.e., N). These processing parameters were examined experimentally to determine the optimal values. The effect of overlapping of adjacent windows was also examined and found to be necessary for optimal performance.

Experimental results indicate that for a fixed bandwidth, the smallest window spacing, which corresponds to the FFT resolution of Δf_A = 98 kHz and Δf_L = 121 kHz in the axial and lateral directions, respectively, produces the best results. Furthermore, it was observed that the optimal window bandwidth must be large enough to prevent significant interference between the target and clutter echos, which is detrimental to performance, but not too large as to yield only minimal clutter decorrelation within the spectral range. Therefore, the optimal bandwidth value reflects a tradeoff between clutter decorrelation and target echo resolution. Fundamentally, the performance will be limited by the effective number of independent windows within the available spectral region.

The choice of window shape, in general, does not significantly affect the performance. Therefore, any suitable window shape may be used including rectangular. However, in practice, Gaussian windows are preferred due to their well-behaved nature in both the time and frequency domains (no sidelobe effects). Furthermore, Gaussian windows are ideal since the transfer function of most typical transducers can be approximated by the Gaussian shape.

The application of the PT algorithm to the SST75 data using optimal window parameters yields the processed data shown in Fig. 2(b). It is clear that the algorithm provides excellent results by removing virtually all the grain noise. The experimental procedures were repeated for the other samples. Fig. 3(a) and (b) shows the wide-band and processed images, respectively, for the SST50 sample which has a 4.2 mm diameter flat-bottom hole located at 67.1 mm depth and an average grain size of 86 μm.

The processed image presented here for the SST75 stainless steel sample is particularly significant since it demonstrates that the PT algorithm is able to distinguish between the high-level grain noise in the unprocessed image (which can easily be mistaken for flaw) and the actual flaw signal, as predicted by the theoretical SNRE calculations. Although nonlinear algorithms such as PT result in excellent SNRE compared to linear techniques, it should be noted that the process may increase the probability of miss, especially when multiple targets are present in the range cell. However, since *B*-scans consist of a large number of closely spaced *A*-scans, there is considerable redundancy which reduces the likelihood of eliminating a target. Therefore, nonlinear algorithms such as PT are more suitable for imaging than *A*-scan applications.

Conclusions

The polarity thresholding algorithm, which is used in conjunction with SSP, has been evaluated both experimentally and theoretically. The algorithm was implemented for 2-D imaging of large grained materials to test its feasibility in practical applications. Experimental results indicate that the choice of window parameters and spectral region are critical to the performance of the algorithm. As expected from the theoretical SNRE derivations, the experimental results provide significant reduction in grain noise, which indicates that the PT algorithm should be highly effective in industrial and medical imaging when significant coherent noise is present.

Acknowledgment

The authors would like to acknowledge the technical assistance of R. Murthy in data acquisition and manuscript preparation.

References

[1] E. W. Beasley and H. R. Ward, "Quantitative analysis of sea clutter decorrelation with frequency agility," *IEEE Trans. Aerosp. Electron. Syst.*, vol. AES-4, pp. 468–473, May 1968.

[2] N. M. Bilgutay, J. Saniie, E. S. Furgason, and V. L. Newhouse, "Flaw-to-grain echo enhancement," in *Proc. Ultrason. Int. 1979*, May 1979, pp. 152–157.

[3] N. M. Bilgutay, U. Bencharit, and J. Saniie, "Nonlinear spectral processing techniques for ultrasonic imaging," in *Review of Progress in Quantitative NDE, Vol. 7-A*, D. Thompson and D. Chimenti, Eds. New York: Plenum, 1988, pp. 757–767.

[4] N. M. Bilgutay, J. Saniie, and U. Bencharit, "Spectral and spatial processing techniques for improved ultrasonic imaging of materials," in *Signal Processing and Pattern Recognition in NDE of Materials*, NATO ASI Ser., vol. F 44, C. H. Chen, Ed. Berlin: Springer-Verlag, 1988, pp. 71–85.

[5] R. Murthy, "Analysis of clutter suppression algorithms in ultrasonic nondestructive testing," M.S. thesis, Drexel Univ., Philadelphia, PA, July 1988.